Available online at www.sciencedirect.com

ScienceDirect

journal homepage: www.elsevier.com/locate/he

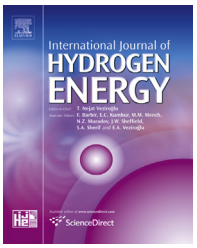

Hydrogen absorption in Ni-catalyzed Mg: A model for measurements in the low temperature range

Federico Cova[*], *Fabiana Gennari*, *Pierre Arneodo Larochette*

Consejo Nacional de Investigaciones Científicas y Técnicas, CONICET, Instituto Balseiro (UNCuyo and CNEA), Centro Atómico Bariloche (CNEA), R8402AGP S. C. de Bariloche, Río Negro, Argentina

ARTICLE INFO

Article history:
Received 26 March 2014
Received in revised form
12 May 2014
Accepted 14 May 2014
Available online 20 June 2014

Keywords:
Kinetic model
Magnesium hydride
Hydrogen storage

ABSTRACT

Magnesium has been deeply studied as a possible hydrogen storage material for both, mobile and static applications. In this article we continued the work presented in our previous paper by modeling the hydrogen absorption in Ni-catalyzed magnesium in the range of pressures of 500 kPa–5000 kPa and temperatures from 423 K to 468 K. A new model based in the Ginstling–Brounshtein diffusion equation was proposed for the hydrogen absorption kinetics. It adds the contribution of the pressure of the gaseous phase and the enthalpy of reaction to the previously mentioned diffusive model. An activation energy for the process was estimated and the value obtained (112 kJ/mol) was concordant with previous values reported in the literature.

Introduction

Due to the actual crisis of energy, the utilization of hydrogen as an energy carrier has attracted a lot of attention from the scientific and technological community. One of the most difficult challenges in order to achieve a feasible hydrogen-based economy is the development of a safe and efficient storage system. Solid-state storage systems have an edge over liquid hydrogen tanks and compressed hydrogen gas because they allow transportation at low pressures and does not require cryogenic temperatures. For a material to be considered as a viable hydrogen carrier, high gravimetric and volumetric hydrogen capacities as well as an adequate thermodynamic stability and fast kinetics are required [1,2]. Among the various materials proposed, magnesium has attracted considerable attention due to its low density, high theoretical gravimetric hydrogen density of 7.6 wt.% and high volumetric hydrogen density (110 kg/m^3) [3–5]. However, MgH_2 is quite stable and its decomposition kinetics is slow at temperatures below 573 K, which impedes its use especially for mobile applications. One of the key problems now for the MgH_2 system is how to improve the kinetic behavior of the hydriding/dehydriding reaction [6,7]. Ni has been proposed as a catalyzer resulting in a great enhancement in the reaction kinetics of the system [8–10]. By adding a 2% molar of Ni to Mg, it was possible to reduce the time needed to complete the hydriding reaction from 300 s to less than 10 s at 573 K [8].

In order to determine the path for future attempts to improve the system, a theoretical quantitative description for hydriding/dehydriding reaction steps is required. However, the model proposed has to be simple enough to be used if necessary in calculations of real-life hydrogen storage tanks. General approaches have been developed trying to model the multiple steps involved in the gas–solid reactions [11–15]. Chou proposed a new model for hydrogen absorption in

* *Corresponding author*. Tel.: +54 294 4445278; fax: +54 294 4445190.
E-mail address: covaf@cab.cnea.gov.ar (F. Cova).
http://dx.doi.org/10.1016/j.ijhydene.2014.05.092

intermetallic systems based on a core–shell structure which could predict the rate limiting step of gas–solid reactions [11]. Chou also proposed a model for hydrogen absorption in systems with slow kinetics (reaction times greater than 500 s) which considers the reacted fraction and the hydrogen partial pressure influence in the hydrogen concentration in the hydride (β) phase [16]. Flanagan et al. [12] proposed various equations for a wide range of reactions, classified in four different subtypes according to the controlling mechanism: nucleation, geometrical contraction, diffusion and reaction-order. Since the models presented by Flanagan were deduced for solid–solid reactions, none of them considers the system pressure influence in the reaction rate. Several authors [13–15] have presented rate equations which depend on the system pressure with different pressure dependence functions but do not consider the effect of the reacted fraction (x), which is defined as the amount of hydrogen absorbed at a given time relative to the amount of hydrogen absorbed at the end of the measurement.

Our previous work [17] showed that the hydrogen absorption rate at temperatures over 478 K was controlled by a single mechanism and adequately described with an experimental three independent contributions (P, T and x) model. This new model will be referred as *ETIC model*. It was also showed in that work, that the heat released by the reaction during the hydriding process has a strong effect on the reaction rate causing an important temperature peak (over 30 K) which also increases the equilibrium pressure. Moreover, we illustrated that hydrogen absorption rate at temperatures between 438 K and 468 K presents a dual behavior. For lower initial pressures, the absorption reactions showed the same mechanism that the low temperature reactions, and at higher pressures they behave like the high temperature ones. It is possible to assume that at intermediate pressures a mechanism transition occurs. In this work the behavior of the samples at low temperature is studied; this includes the intermediate temperatures and low pressure ranges where the low temperature mechanism is present. In order to find the model that fits the experimental data, a simplified approach of the one used in our previous work will be applied, considering the reaction rate variation with temperature, pressure and reacted fraction. These considerations lead to the following equation for the reaction rate r:

$$r = \frac{dx}{dt} = kf(x)h(P) \tag{1}$$

In this equation, $f(x)$ represents the formula for the reaction model as proposed by Flanagan [12], k is the reaction rate constant which includes the dependence with the temperature of the model and $h(P)$ is the contribution to the reaction rate given by the pressure. The addition of the $h(P)$ to the models proposed by Flanagan is necessary to consider the influence of the reactive in gaseous phase. For the hydrogen absorption in Ni-catalyzed magnesium it is very important to take the hydrogen pressure into account to calculate the reaction rate.

In addition, the models proposed by Flanagan do not take the heat released during the reaction into account [18]. While this assumption may be true for solid state reactions, the magnesium reaction with hydrogen is highly exothermic, and this effect should not be underestimated. In order to consider the thermal effects, equation (2) has been proposed for the temperature variation with time [17]:

$$\frac{dT}{dt} = \left(\frac{\Delta H}{C_P}\frac{dx}{dt} - k_T(T - T_{SP})\right) \tag{2}$$

in which k_T is a dissipation factor and T_{SP} is the temperature outside the reactor. A similar model has been proposed by Lozano et al. [19] for the $NaAlH_4$ system, although this system has a much lower reaction enthalpy and thus it was possible to keep the temperature outside the reactor wall constant. This equation is only accurate when the Biot number of the system is much smaller than 1. In the present case, the value obtained for the Biot number is between 2 10^{-4} (if the system includes the Cu sample holder) and 10^{-3} (considering only the MgH_2 sample as the system). These values allowed to consider the equation (2) as an acceptable model for the studied system.

In this work, the models proposed by Flanagan are used as a point of departure and are then modified to take pressure changes and thermal effects into account. Having a simple equation that describes adequately the behavior of the system and allow modeling its behavior is fundamental for the design of solid-state based hydrogen storage tanks.

Experimental

The samples were prepared by milling a mixture of MgH_2 (Sigma–Aldrich; hydrogen storage grade) and 2% molar Ni (Alfa Aesar; powder mesh <300). The milling was performed under Ar atmosphere at 400 rpm for 10 h in a Fritsch Pulverisette 6 planetary mill with stainless steel vial and balls. The ball/sample weight ratio selected was 40:1. All the sample manipulation was handled in an Ar-filled glove box equipped with a purification system, in which the typical H_2O/O_2 levels were below 1 ppm.

The absorption kinetics measurements were performed in a Sieverts-like device, at constant temperatures varying from 423 K to 468 K and an initial pressure range from 500 kPa to 5000 kPa. These parameters were selected because the results of our previous work [17] showed that the behavior of the system has a controlling mechanism transition in this range of pressure and temperature. A scheme of the device, indicating the thermocouple location is shown in the same article. It is possible to notice that the sample holder and the thermocouple are separated by stainless steel wall. This configuration is the most common in this kind of devices and is the easiest to scale up to a storage tank.

A sample holder with central mass made of Cu, was used for the measurements. This sample holder presents two important advantages, first it allows the sample to be distributed in a ring shape improving the heat dissipation through the holder walls, and second the central Cu mass acts as a thermal buffer absorbing part of the heat released. The Cu sample holder has a mass of 10 g while the sample had a mass of 0.15 g.

Due to the sudden expansion of the hydrogen at the beginning of each experiment and the fast kinetics of absorption reaction it is very difficult to obtain a first measured point without an inherent error. The first measured pressure

could be different from the real one due to effects of the fluid dynamics. To correct this effect, all absorption curves were processed by adjusting the first point so that the final capacity of the absorption matches the capacity of the subsequent experiment of hydrogen desorption. The initial measured pressure was replaced with an estimated one. This pressure was calculated to guarantee that at the end of the reaction process, the amount of absorbed hydrogen matches the hydrogen released in the following desorption.

A genetic algorithm was used as a parameter adjusting method. This algorithm takes at random a population of possible parameters and evaluates its goodness of fit. Then it creates a new generation of parameters by mixing the ones which best fitted the previous generation. In this way, with each generation, the population "evolves" to better results. In this case, an initial population of 200 individuals was selected and it evolved for 30 generations.

The criterion used to determine the goodness of fit of the calculated curves and the experimental data is the squared correlation coefficient (R^2) which reflects the level of agreement between the fitting curve and the measured points. The expression for R^2 is presented in equation (3):

$$R^2 = \frac{\left(N\sum_{i=1}^{N}\left(y_i^{exp}\cdot y_i^{calc}\right)-\sum_{i=1}^{N}\left(y_i^{exp}\right)\cdot\sum_{i=1}^{N}\left(y_i^{calc}\right)\right)^2}{\left(N\sum_{i=1}^{N}\left(y_i^{exp}\right)^2-\left(\sum_{i=1}^{N}\left(y_i^{exp}\right)\right)^2\right)\cdot\left(N\sum_{i=1}^{N}\left(y_i^{calc}\right)^2-\left(\sum_{i=1}^{N}\left(y_i^{calc}\right)\right)^2\right)} \quad (3)$$

where y_i^{exp} is the measured experimental data i, y_i^{calc} is the value calculated from the model that corresponds to the experimental point i, and N is the number of experimental data points. R^2 values vary from 0 to 1, a value close to 1 indicates a good agreement between the model and the experimental data. The model which has its R^2 value closer to 1 is the one that better represents the experimental data, and thus will be considered the most adequate.

Results and discussion

The hydrogen reaction kinetics of the samples was obtained by continuous cycling in the Sieverts device. The samples show good stability after several absorption/desorption cycles and have a storage capacity of 5.4 wt. % (instead of the theoretical value of 7.2 wt. %) due to the difficulty for the hydrogen to reach the core of the magnesium particle. The microstructural properties of the material were studied by XRD and SEM techniques and the results showed that the system consisted in a mixture of Mg/MgH_2 with small amounts of Ni and Mg_2Ni/Mg_2NiH_4 which acts as catalyzers [8].

Fig. 1A shows the hydrogen absorption curves for different temperatures and at an initial pressure of 3000 kPa. As it is expected the reaction needs more time to be completed at lower temperatures.

The reaction rate for every data point in the measurements was calculated by a finite difference method, using the slope of the secant between the two closest points (the previous and the following). In Fig. 1B the reaction rate dependence with the pressure is shown for the different studied temperatures. In this figure it is possible to notice the rise of the rate that occurs for certain temperatures when the system pressure reaches the mechanism transition pressure. The two lowest temperatures (423 K and 428 K) do not show a change in the reaction mechanism. During the absorptions, the volume kept at room temperature was much bigger (26 cm^3) than the volume at high temperature (2 cm^3), the difference between the initial pressure and the final temperature was approximately constant (300 kPa) for all the measurements done. For this reason the initial pressure was utilized as reference for the measurements.

In an attempt to determine the mechanism that controls the reaction rate, the linearized models proposed by Flanagan [12] were fitted to the experimental data with a least squares method and the R^2 was calculated for every measurement in the studied range of pressures and temperatures.

Fig. 2 shows the average value of the R^2 parameter for each of the models proposed by Flanagan. This average was done using the values obtained for the R^2 parameter of the measurements in the temperature and pressure regions without a mechanism change.

From this figure it is possible to notice that the diffusion control models are the most accurate for describing the absorption reaction. All four diffusion models showed a good

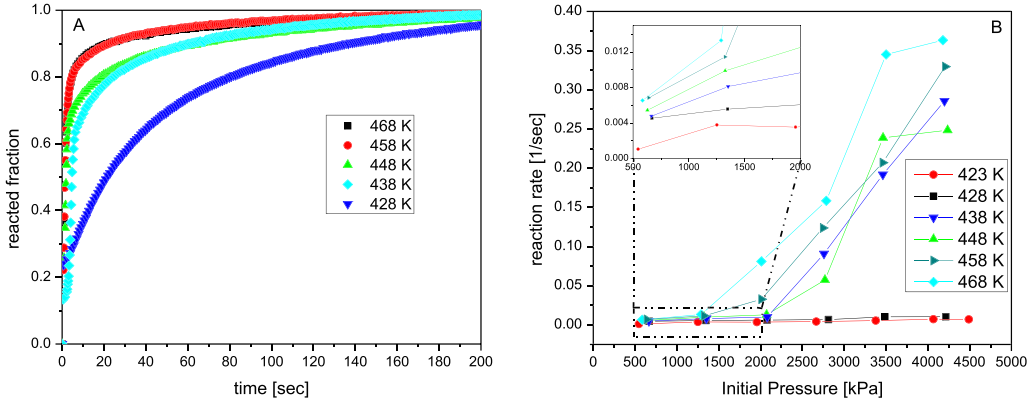

Fig. 1 – Hydrogen absorption curves for different temperatures at an initial pressure of 3000 kPa (A) and reaction rate dependence with pressure for different pressures and temperatures at a reacted fraction value of 0.5 (B). The insert presents the low pressure region.

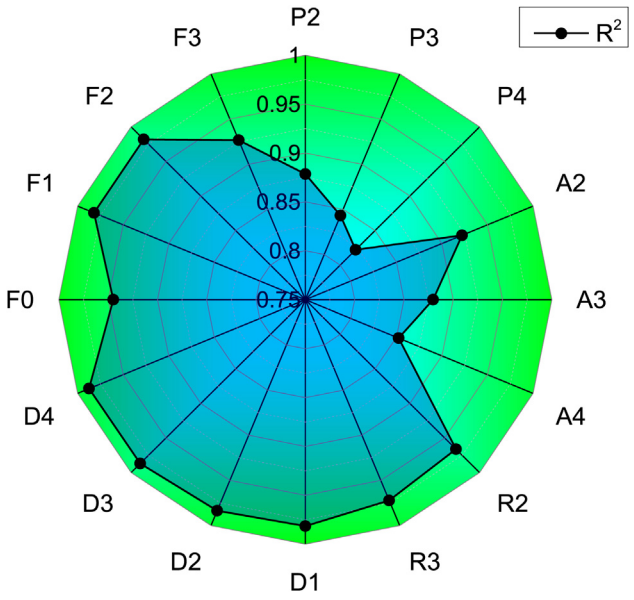

Fig. 2 – Average R^2 of the different models proposed by Flanagan. (P: Polynomial. A: Avrami, R: Geometric contraction, D: Diffusion, F: Reaction order) [12].

fitting of the experimental absorption curves. The equations corresponding to these models are shown in Table 1.

A plot of the integral form as a function of time provides an easy method to determine the goodness of fit of the models by studying the deviation of the $g(x)$ from a linear function through its R^2 parameter. On the other side, the differential form $f(x)$ determines the reaction rate dependence with the reacted fraction.

In order to determine which of the four equations should be used for the simulations, the $g(x)$ functions proposed by Flanagan [12] were calculated for each curve and normalized using the value of the curve at 200 s. This value was selected because it is the time at which all the absorptions have reached their maximum capacity. The normalization allowed the direct comparison between the different models. The results of these calculations are shown in Fig. 3; the hollow symbols show the average value of the normalized function for all the measurements and the colored areas enclose the variation range of the normalized function. The reference dashed line shows the expected behavior for a perfectly accurate model.

From this figure it is very clear that the best fitting models are the Jander (D3) and the Ginstling–Brounshtein (D4); both models describe three dimensional diffusion in spherical particles [20–22]. These results are consistent with the assumption about the reduced capacity of the system. The slow diffusion through the outer layer of magnesium hydride limits the capacity of the hydrogen to reach the inner magnesium core of the particles resulting in an absorption capacity which is lower than the theoretical one. This effect occurs at both, low and high temperature ranges, but diffusion is the step that controls the absorption rate in the low temperature range.

Although the chosen models showed a good fitting of the experimental data, it is important to realize that, as previously stated, all of them were developed for solid state reactions and do not take the pressure of the reactive in gaseous phase into account. In order to find out the hydrogen pressure influence in the reaction rate, in Fig. 4 the resulting value for the parameter k for different measurements has been plotted against the initial system pressure.

In this figure is possible to notice that the parameter k for both of the preferred models has a similar behavior, which can be approximated as linear. As the reaction rate is proportional to the parameter k, and this parameter is proportional to the system pressure, it is possible to modify the models proposed in Table 1 to be able to reproduce the absorption curves under variable pressure conditions. Different pressure dependence equations [15] including the equilibrium pressure were also considered. Due to the small variation presented by the equilibrium pressure in the studied temperature range (1.0 kPa at 423 K–4.5 kPa at 468 K), the fittings obtained were similar to the calculated without taking equilibrium pressure into account, and for simplicity, the linear dependence model for the pressure was selected.

Both Jander and Ginstling–Brounshtein equations use a quasi-stationary approach to solve the case of an advancing reaction interface in spherical particles considering the diffusion through the shell as the limiting step. From this is possible to conclude that, since both equations are different solutions for the same problem, the reaction is effectively controlled by diffusion. Between these two models is not possible to determine which one is better from the measured curves because the best fit is not always the same in every absorption curve. In order to solve this problem it is important to consider the limitations of the models established in the literature. Harrison suggested that Jander equation should not be trusted for x beyond 0.15 while Ginstling–Brounshtein could be applied up to high values of x in practical circumstances [22]. For this reason the model selected is the proposed by Ginstling and Brounshtein.

With the selected model, all the measured curves were fitted, including the ones which showed a mechanism change. The R^2 values dependence with temperature and pressure corresponding to these fittings is shown in Fig. 5.

Table 1 – Reaction rate expressions for the different diffusion models.

Model	Differential form $f(x) = \frac{1}{k}\frac{dx}{dt}$	Integral form $g(x) = kt$
D1: 1D diffusion	$\frac{1}{2}x$	x^2
D2: 2D diffusion	$\frac{1}{-\ln(1-x)}$	$(1-x)\ln(1-x)+x$
D3: 3D diffusion – Jander equation	$\frac{3(1-x)^{2/3}}{2(1-(1-x)^{1/3})}$	$(1-(1-x)^{1/3})^2$
D4: 3D diffusion – Ginstling–Brounshtein equation	$\frac{3}{2((1-x)^{-1/3}-1)}$	$1-\frac{2}{3}x-(1-x)^{2/3}$

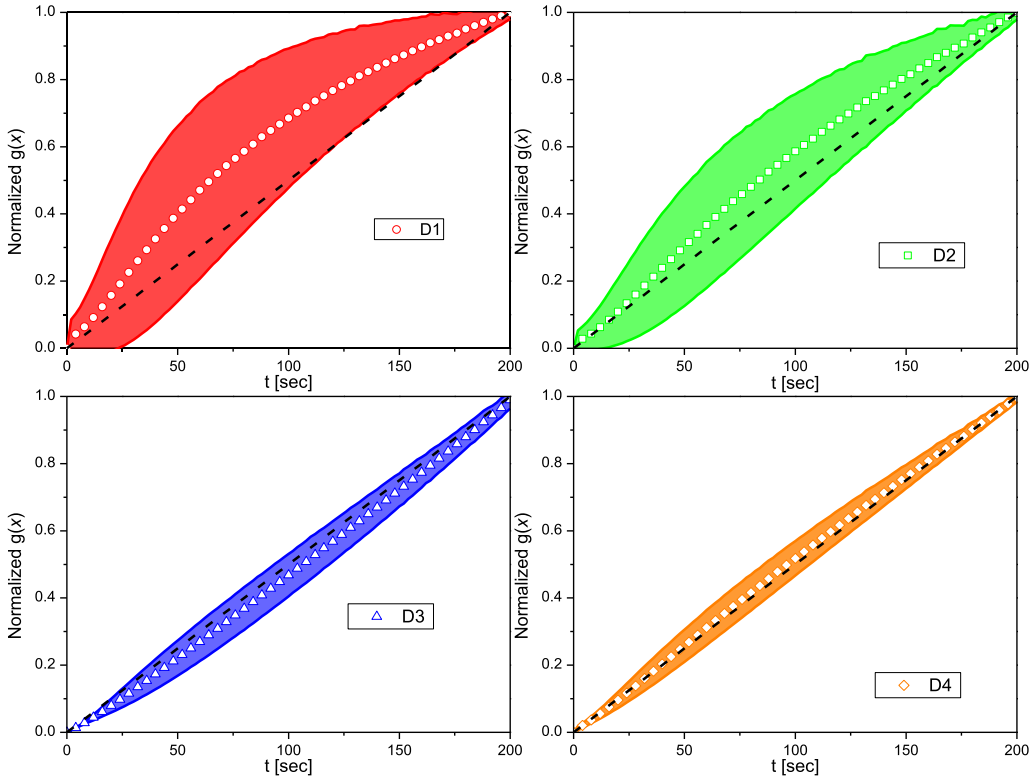

Fig. 3 – Normalized *g*(*x*). Average value (hollow symbols) and range of variation (colored area).

The surface plotted in Fig. 5 shows that the Ginstling–-Brounshtein diffusion model accuracy abruptly decays. While the raise in the reaction rates shown in Fig. 1B could be initially attributed to a raise in the parameter *k*, the R^2 variation showed in Fig. 5 evidences that a mechanism change occurs in this region because the diffusion models proposed were not adequate to describe the behavior of the system at these pressures and temperatures.

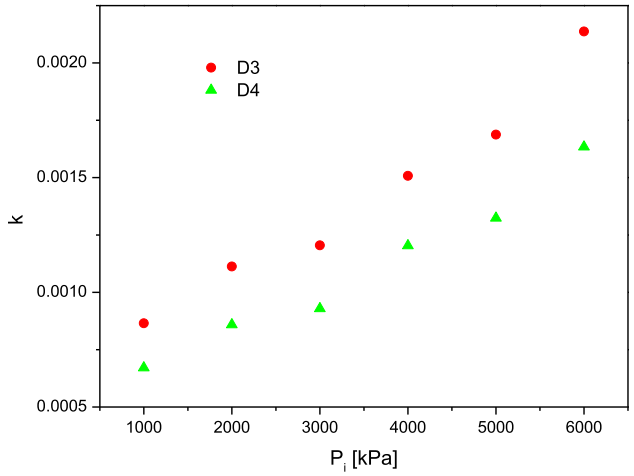

Fig. 4 – Dependence of the parameter *k* with the initial pressure of the system. D3 corresponds to Jander equation and D4 corresponds to Ginstling–Brounshtein equation.

The temperature effect in the reaction rate is given by the dependence of the reaction rate constant, *k*, which is usually assumed to respond to the Arrhenius equation [18] :

$$k = Ae^{\frac{-E_a}{R_g T}} \tag{4}$$

where A is the pre-exponential factor, E_a is the activation energy of the process and R_g is the ideal gas-law constant.

To obtain the value of the activation energy, the reaction rate was calculated for every measurement at a reacted fraction value of 0.5 and a pressure of 1500 kPa for different temperatures. These values were plotted as reaction rate logarithm against the inverse of the temperature. Fig. 6 shows that the experimental data are accurately fitted by a linear function. It was possible to obtain from the slope of the linear function a value for the activation energy of 112 kJ/mol of H_2 was obtained. This value is in agreement with some previously reported for the hydrogen absorption in magnesium in the literature [23,24].

The value obtained is higher than the one calculated for the high temperature range with the *ETIC model* in our previous work (92 kJ/mol). This is an expected result, because higher energy implies a slower process at low temperatures, making diffusion the controlling process. At higher temperatures, the activation energy barrier becomes easier to surpass and other reaction steps become more significant [17].

Taking all these considerations into account, the reaction rate can be written as follows:

$$\frac{dx}{dt} = Ae^{\frac{-E_a}{RT}} P \frac{3}{2\left((1-x)^{-1/3}-1\right)} \tag{5}$$

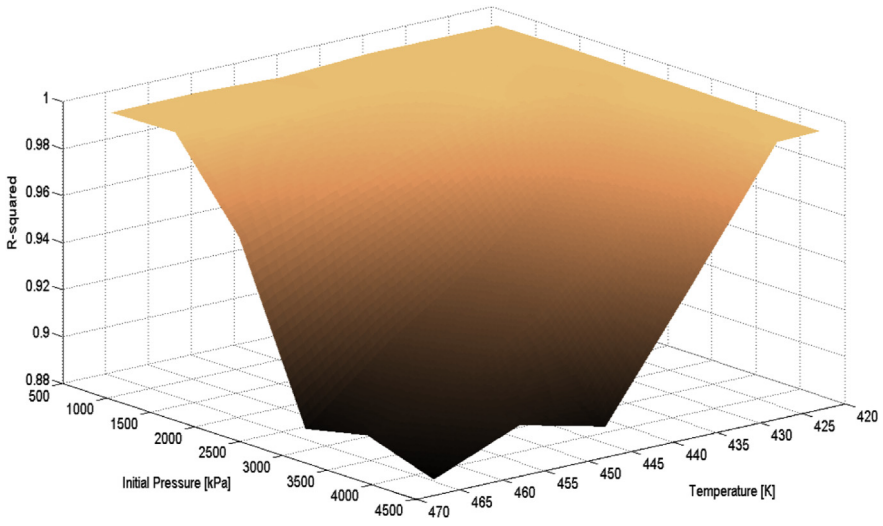

Fig. 5 – R^2 of the Ginstling–Brounshtein model fittings as a function of pressure and temperature.

The temperature dependence is given by equation (2).

$$\frac{dT}{dt} = \left(\frac{\Delta H}{C_P}\frac{dx}{dt} - k_T(T - T_{SP})\right)$$

Using this two equations system, the hydrogen absorption curves were simulated, fitting the parameters A and k_T.

The results of these simulations compared with some of the experimental curves are shown in Fig. 7A, C and E. In Fig. 7B, D and F, the calculated internal temperature and the external measured temperature change is plotted. The delay observed between external and internal temperature peaks can be attributed to the equipment time of response. Results obtained in an independent measurement showed that the time constant of the Sieverts device is 37 s, which is very similar to the delay observed between the temperature peaks (average value of 39.5 s). As can be seen, the proposed model reproduces accurately the experimental absorption behavior. Similar results can be achieved using the Jander equation for the reacted fraction dependence and making the same corrections to include the pressure of the reactive in gaseous phase and the heat released during the reaction; these results are not shown for the previously stated theoretical considerations.

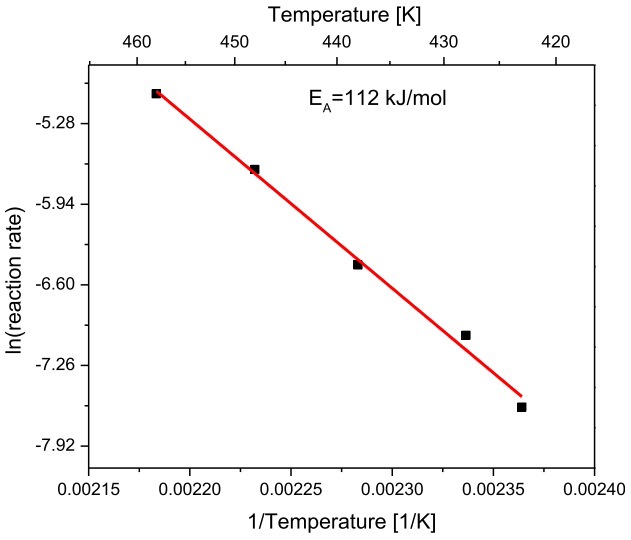

Fig. 6 – Natural logarithm of the reaction rate against the inverse of the temperature. The slope of the linear fit is the activation energy for the process.

It is possible to notice that the highest temperature peak in these cases represents less than 20% of the highest temperature raise that occurs in the high temperature range [17]. This difference can be explained considering the much slower kinetics of the diffusion controlled process that occurs at low temperatures. This slow kinetics allows the system to remove the heat produced by the reaction through the reactor wall.

As a summary, Fig. 8 presents a map that describes the results obtained in the present work (low temperature range) and our previous article (high temperature range). This map shows a representation of the reaction rate controlling mechanism in each region. Two different zones can be easily identified in this map, in correlation with Fig. 1B. At lower pressures and temperatures the reaction controlling mechanism is the diffusion through the magnesium hydride layer. At higher temperatures, the *ETIC model* is the one which describes the process. In between these two regions the mechanism transition occurs. The map presented in Fig. 8 illustrates the difficulty of modeling a real storage material when pressure and temperature are taken into account, even in a very simple system like Ni-catalyzed magnesium.

Conclusions

In this work we concluded the study done in our previous article [17]. The hydrogen absorption in Ni-catalyzed magnesium was studied in the low temperature range. By proposing

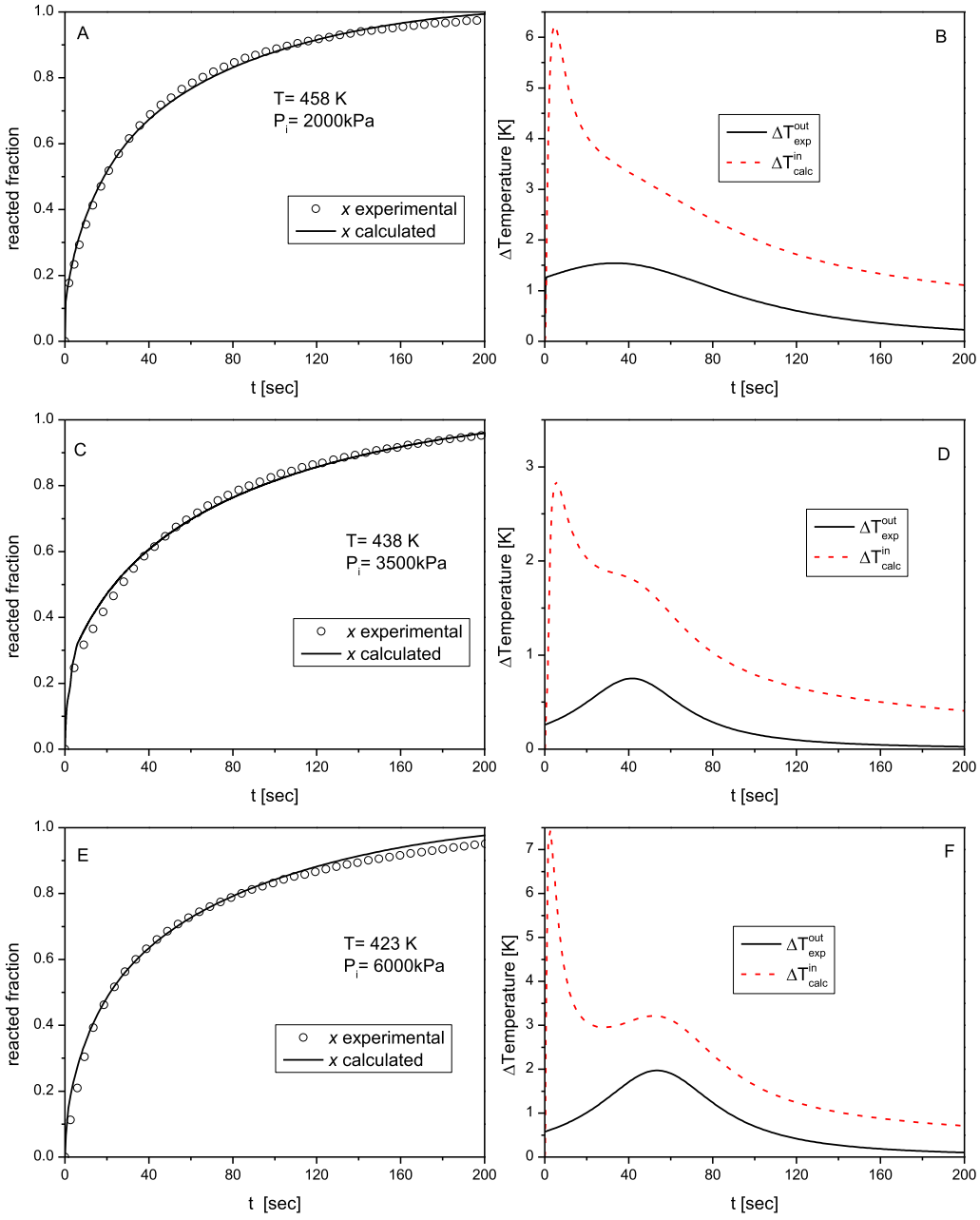

Fig. 7 – Experimental (circles) and simulated (line) hydrogen absorption curves (A, C and E), and changes in the temperatures calculated inside the reactor (red dashed) and measured outside the reactor (black full) (B, D and F). (For interpretation of the references to colour in this figure legend, the reader is referred to the web version of this article.)

and fitting several model equations, it was possible to determine that three dimensional diffusion is the mechanism which controls the reaction. It was also possible to determine the activation energy for the process, which has a reasonable value. The activation energy obtained is more than 20% higher than the calculated in our previous article for the high temperature range.

A correction to the model to take pressure variation into account was introduced and the same thermal behavior considerations done in our previous article was included for the absorption simulations. This modified model was able to reproduce with high accuracy the behavior of the system for the temperature range studied. This permitted to notice that the thermal effects at low temperatures are much smaller than at high temperatures due to the slower absorption kinetics.

It was also possible to determine that a mechanism change occurs at intermediate temperatures and pressures, allowing to differentiate two clearly defined regions, each controlled by different mechanisms and a transition zone in between them.

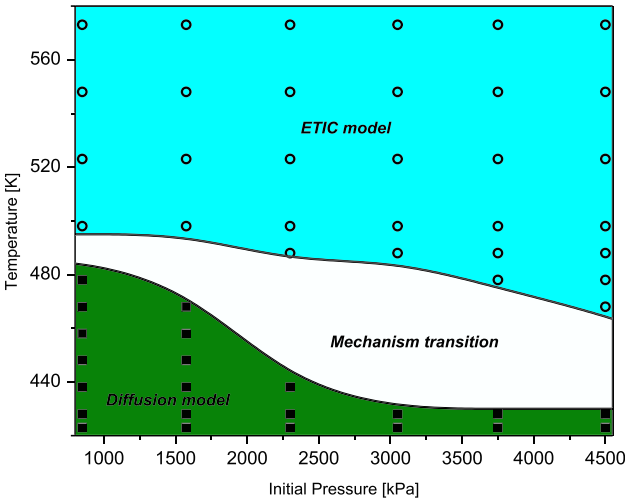

Fig. 8 – Map describing the reaction mechanism for the hydrogen absorption in Ni-catalyzed magnesium. The full squares correspond to the experimental conditions in which the absorption was adequately fitted with the modified diffusion model. The hollow circles correspond to the conditions in which the absorption was adequately fitted with the *ETIC model* in our previous article [17]. The conditions in which absorption could not be fitted are not shown.

Acknowledgments

This study has been partially supported by CONICET (National Council of Scientific and Technological Research), CNEA (National Commission of Atomic Energy), ANPCyT (PICT N° 1049) and Instituto Balseiro (University of Cuyo).

REFERENCES

[1] Züttel A, Borgschulte A, Schlapbach L. Hydrogen as a future energy carrier. Wiley-VHC; 2008.
[2] Walker GS. Solid-state hydrogen storage. Woodhead Publishing Limited; 2008.
[3] Hoffman KC, Reilly J, Salzano FJ, Waide CH, Wiswall RH, Winsche W. Metal hydride storage for mobile and stationary applications. Int J Hydrogen Energy 1976;1:133–51.
[4] Shang CX, Bououdina M, Song Y, Guo ZX. Mechanical alloying and electronic simulations of (MgH_2+M) systems (M=Al, Ti, Fe, Ni, Cu and Nb) for hydrogen storage. Int J Hydrogen Energy 2004;29:73–80.
[5] Selvam P, Viswanathan B, Swamy CS, Srinivasan V. Magnesium and magnesium alloy hydrides. Int J Hydrogen Energy 1986;11:169–92.
[6] Li Q, Lin Q, Chou K, Jiang L, Zhan F. Hydrogen storage properties of mechanically alloyed Mg-8 mol% $LaNi_{0.5}$ composite. J Mater Res 2004;19:2871–6.
[7] Li Q, Chou K, Lin Q, Jiang L, Zhan F. Influence of the initial hydrogen pressure on the hydriding kinetics of the $Mg_{2-x}Al_xNi$ (x=0,0.1) alloys. Int J Hydrogen Energy 2004;29:1383–8.
[8] Cova F, Arneodo Larochette P, Gennari F. Hydrogen sorption in MgH_2-based composites: the role of Ni and $LiBH_4$ additives. Int J Hydrogen Energy 2012;37:15210–9.
[9] Wronski ZS, Carpenter GJC, Czujko T, Varin RA. A new nanonickel catalyst for hydrogen storage in solid-state magnesium hydrides. Int J Hydrogen Energy 2011;36:1159–66.
[10] Jensen TR, Andreasen A, Vegge T, Andreasen J, Stahl K, Pedersen A, et al. Dehydrogenation kinetics of pure and nickel-doped magnesium hydride investigated by in situ time-resolved powder X-ray diffraction. Int J Hydrogen Energy 2006;31:2052–62.
[11] Chou K-C, Xu K. A new model for hydriding and dehydriding reactions in intermetallics. Intermetallics 2007;15:767–77.
[12] Khawam A, Flanagan DR. Solid-state kinetic models: basics and mathematical fundamentals. J Phys Chem B 2006;110:17315–28.
[13] Martin M, Gommel C, Borkhart C, Fromm E. Absorption and desorption kinetics of hydrogen storage alloys. J Alloy Compd 1996;238:193–201.
[14] Forde T, Maehlen J, Yartys V, Lototsky M, Uchida H. Influence of intrinsic hydrogenation/dehydrogenation kinetics on the dynamic behaviour of metal hydrides: a semi-empirical model and its verification. Int J Hydrogen Energy 2007;32:1041–9.
[15] Ron M. The normalized pressure dependence method for the evaluation of kinetic rates of metal hydride formation/decomposition. J Alloy Compd 1999;283:178–91.
[16] Chou K-C, Li Q, Lin Q, Jiang L, Xu K. Kinetics of absorption and desorption of hydrogen in alloy powder. Int J Hydrogen Energy 2005;30:301–9.
[17] Cova F, Gennari F, Arneodo Larochette P. Numerical modeling of hydrogen absorption measurements in Ni-catalyzed Mg. Int J Hydrogen Energy 2014;39:5010–8.
[18] Khawam A, Flanagan DR. Role of isoconversional methods in varying activation energies of solid-state kinetics II. Nonisothermal kinetic studies. Thermochim Acta 2005;436:101–12.
[19] Lozano GA, Ranong CN, Bellosta von Colbe JM, Bormann R, Fieg G, Hapke J, et al. Empirical kinetic model of sodium alanate reacting system (I). Hydrogen absorption. Int J Hydrogen Energy 2010;35:6763–72.
[20] Jander W. Reaktionen im festen Zustande bei höheren Temperaturen. Reaktionsgeschwindigkeiten endotherm verlaufender Umsetzungen. Z Anorg Allg Chem 1927;163:1–30.
[21] Segal E. Rate equations of solid state reactions. Euclidean and fractal models. Rev Roum Chim 2012;57:491–3.
[22] Bamford CH, Tipper CFH. Chemical kinetics. vol. 2. The theory of kinetics. Elsevier Scientific Publishing Company; 1969.
[23] Kojima Y, Kawai Y, Haga T. Magnesium-based nano-composite materials for hydrogen storage. J Alloy Compd 2006;424:294–8.
[24] Mao J, Guo Z, Yu X, Liu H, Wu Z, Ni J. Enhanced hydrogen sorption properties of Ni and Co-catalyzed MgH_2. Int J Hydrogen Energy 2010;35:4569–75.